Journal of Astronomical Telescopes, Instruments, and Systems

AstronomicalTelescopes.SPIEDigitalLibrary.org

All-sky survey mission observing scenario strategy

Sara C. Spangelo
Raj M. Katti
Stephen C. Unwin
Jamie J. Bock

SPIE.

All-sky survey mission observing scenario strategy

Sara C. Spangelo,[a,*] Raj M. Katti,[b] Stephen C. Unwin,[a] and Jamie J. Bock[a,b]
[a]California Institute of Technology, Jet Propulsion Laboratory, 4800 Oak Grove Drive, Pasadena, California 91109, United States
[b]California Institute of Technology, MC 249-17, 1200 East California Boulevard, Pasadena, California 91125, United States

Abstract. This paper develops an observing strategy for space missions performing all-sky surveys, where a single spacecraft maps the celestial sphere subject to realistic constraints. The strategy is flexible, accommodates targeted observations of specific areas of the sky, and achieves the desired trade-off between survey goals. This paper focuses on missions operating in low Earth orbit with interactive and dynamic thermal and stray-light constraints due to the Sun, Earth, and Moon. The approach is applicable to broader mission classes, such as those that operate in different orbits or that survey the Earth. First, the instrument and spacecraft configuration is optimized to enable visibility of the targeted observations throughout the year. Second, a constraint-based strategy is presented for scheduling the observations throughout the year subject to a simplified subset of the constraints. Third, a heuristic-based scheduling algorithm is developed to assign the all-sky observations over short planning horizons. The constraint-based approach guarantees solution feasibility. The approach is applied to the proposed SPHEREx mission, which includes coverage of the north and south celestial poles, galactic plane, and a uniform coverage all-sky survey that maps the entire celestial sphere twice per year. Visualizations demonstrate how the all-sky survey achieves its redundancy requirements over time. [DOI: 10.1117/1.JATIS.1.3.037001]

Keywords: all-sky survey; observing strategy; scheduling; SPHEREx.

Paper 14030 received Nov. 3, 2014; accepted for publication Jul. 6, 2015; published online Aug. 7, 2015.

1 Introduction

1.1 *Observing Scenario Overview*

This paper develops an observing strategy for accomplishing an all-sky survey with targeted observations with a space-based observatory. The approach is applicable to spacecraft missions mapping both the celestial sphere (zenith-pointing) and the Earth (nadir-pointing). The approach focuses on missions in a low Earth orbit (LEO), although the constraints can be modified or relaxed and applied to a broader range of orbit scenarios. The observing problem is dynamic throughout the year as the orbit evolves relative to the Sun, Moon, celestial sphere, and potential targets (e.g., galactic plane). The problem formulation considers interacting and dynamic constraints related to thermal and stray-light avoidance relative to the Sun, Earth, and Moon for a mission operating in LEO. These combined constraints limit the zone where the spacecraft and instrument can point, which varies throughout the year. Decisions related to both to the spacecraft configuration and observing strategy, which must be robust throughout the full year, are addressed. System-level issues related to the spacecraft configuration, the telecommunication system, the attitude control system, and the thermal control system are considered in the strategy. The scheduling algorithm is applied to the SPHEREx astrophysics mission, which includes an all-sky survey, galactic-plane survey, and survey targeting the celestial poles.

1.2 *Literature Review*

There is a large body of related research on spacecraft operations and scheduling related to the problem addressed in this paper. Most of the scheduling approaches described in the literature involve a nadir-pointing spacecraft; however, many of the formulations in the literature share similar dynamics, constraints, and objectives with the observing problem addressed in this paper. We review the historic space-based all-sky survey observatories and scheduling work for other related missions and discuss their similarities and differences relative to the problem addressed in this paper.

Several space-based observatory missions performed or proposed all-sky surveys. The infrared astronomical satellite (IRAS) was the first space-based observatory to perform a survey of the sky at infrared wavelengths from LEO.[1] IRAS mapped 96% of the sky with a focal plane with detectors at four wavelengths. The IRAS satellite design and survey strategy were optimized to maximize the detection of point sources.[2] IRAS mapped out "lunes" bounded by ecliptic meridians separated by 30 deg. The Akari infrared astronomy satellite surveyed the entire sky in the near-, mid-, and far-infrared from LEO.[3] This mission achieved full sky coverage by pointing the instrument in the zenith direction and continuously scanning the sky, where observations were constrained by the Sun and Earth.[4] Akari scanned 94% of the sky twice and performed 5000 pointed observations within approximately 1.5 years following launch. Wide-field infrared survey explorer (WISE) performed an all-sky survey from LEO.[5] WISE's observing scenario consisted of pointing approximately in the zenith and scanning lines of constant ecliptic longitude. WISE surveyed

*Address all correspondence to: Sara Spangelo, E-mail: Sara.Spangelo@jpl.nasa.gov

2329-4124/2015/$25.00 © 2015 SPIE

the whole sky in 6 months, taking a 47-arcminute field-of-view (FOV) image every 11 s.[6] The ROSAT mission operated in LEO, where the observing strategy consisted of scanning a 0.5 deg FOV along great circles to cover 6.4 deg ×6.4 deg tiles, where a total of 1378 tiles covered the sky.[7] The Transiting Exoplanet Survey Satellite (TESS) mission will monitor the full celestial sphere in a two-year mission. The instrument FOV steps 27 deg east every 27 days from a high Earth orbit in a 2:1 resonant orbit with the Moon.[8] Most of the existing all-sky observing strategies used a step-and-stare approach with a zenith-pointed instrument, and most also did not consider targeting in addition to the all-sky survey.

There has been considerable scheduling work for pointed space-based observatories which is informative in the development of all-sky scheduling algorithms. The Hubble Space Telescope (HST), launched in 1990, resulted in one of the largest and most complex scheduling problems, with 10,000 to 30,000 observations to be annually scheduled. Hubble operated in the challenging LEO environment and as a result was subject to a large number of operational and scientific constraints.[9] HST scheduling problems were formulated as constraint satisfaction problems and solved with search approaches that include multi-start stochastic repair strategies. The James Webb Space Telescope (JWST), HST's successor, which is planned to be launched in 2018, will operate from Earth–Sun L2 and is also a complex multiobjective scheduling problem. JWST scheduling problems have three objectives: to minimize schedule gaps, to minimize the number of observations that miss their last scheduling opportunity, and to minimize momentum build-up. JWST problems are solved using evolutionary algorithms.[10,11]

This paper presents a scheduling approach for all-sky surveys that can accommodate targeted observations. Most observing problems in the literature consist of a zenith-pointing spacecraft with an efficient simple scanning strategy and it is not clear how these solutions accommodate targeted observations. Furthermore, most existing strategies are not restricted by dynamic thermal and stray-light constraints, nor do they consider instrument and spacecraft configuration decisions. In general, the formulations and approaches in the literature have a different set of problem objectives, decisions, and constraints relative to the all-sky survey considered in this paper.[1–11] This paper develops a strategy for accomplishing an all-sky survey with targeted observations near the celestial poles and applies it to the SPHEREx astrophysics mission. Much of the observatory scheduling literature is informative in developing these models and algorithms.

1.3 *Paper Overview*

The observing scenario problem constraints and objectives are described in detail in Sec. 2. Capturing this problem as a single formulation problem would be complex and it would be difficult to generate solutions that are guaranteed to be feasible. To overcome this challenge, this paper separates and solves this problem in series, passing a simplified set of constraints between subproblems. Thus, although solutions may not be guaranteed optimal (for an objective function such as maximizing science efficiency), they are guaranteed to be feasible and satisfy all orbit, spacecraft, instrument, and mission requirements. First, a feasible instrument configuration is established that satisfies the Sun-avoidance constraint and observability requirements throughout the year. Second, the configuration and Earth-avoidance constraints are combined to determine the maximum observation time constrained by the angle of the orbital plane relative to the Sun. These first two steps are described in Sec. 3.1. Third, a high-level scheduling strategy and a resultant constraint-based heuristic algorithm are developed in Sec. 3.2. Section 4 applies the scheduling algorithm to the SPHEREx, an astrophysics LEO mission that includes three surveys with variable requirements, including an all-sky survey. The survey goals are achieved with the scheduling approach presented and demonstrated with coverage visualizations. The contributions and results are summarized and insights into how the step-wise approach presented in this paper can be applied to other observing scenarios are described in Sec. 5.

2 Problem Description

This section describes the all-sky scheduling problem by defining vectors, angles, constraints, and then defining scheduling terms used throughout the paper. It is assumed that the spacecraft is in a Sun synchronous LEO, as typically selected for all-sky surveys, such as IRAS, Akari, and WISE. Missions with different orbits may still benefit from the algorithms in Sec. 3, but may require alternative formations of the constraints (for most other orbits, many of the constraints can be relaxed or ignored as LEOs tend to be particularly constraining). In a Sun synchronous orbit, every Earth rotation provides visibility to all declinations of the celestial sphere. By definition, Sun-synchronous orbits precess at a rate of approximately 1 deg a day; thus the instrument has access to the entire celestial sphere approximately every 6 months.

The overall goal of the scheduling problem is to efficiently perform an all-sky survey of the celestial sphere and perform targeted observations. The decision variables are where and when to point the instrument on the celestial sphere as a function of time. The dynamics include the orbital motion and constraints related to the thermal and stray-light avoidance from the Earth, Sun, and Moon.

Prior to describing the constraints, several vectors and angles are defined:

- Spacecraft $+Z$ axis: symmetry axis of the spacecraft.
- Instrument boresight: vector aligned with the center of the telescope FOV.
- Beta angle (β): the angle between the orbital plane and vector to the Sun.
- Tilt angle (θ): the angle between the orbital plane and the spacecraft $+Z$ axis in the orbital cross-track direction.
- Cant angle (ϕ): the angle between the spacecraft $+Z$ axis and the instrument boresight in the orbit in-track direction.
- Nod angle (δ): the angle between the spacecraft $+Z$ axis and the local zenith in the orbital plane.

The scheduling problem is also subject to the following spacecraft and instrument constraints (where the angles are shown in Fig. 1):

- Sun-avoidance criteria: spacecraft $+Z$ axis cannot be pointed within Ω of the vector to the Sun due to thermal constraints, which place the constraint on tilt angle:

$$\theta \geq \Omega - \beta. \tag{1}$$

- Earth-avoidance criteria: spacecraft $+Z$ axis cannot be pointed more than α from the local zenith due to thermal constraints. The spacecraft is rotated both in the cross-track

direction by θ and the in-track direction by δ; thus the constraint on the resulting total angle from local zenith is:

$$\cos(\alpha) = \cos(\theta)\cos(\delta). \tag{2}$$

- Moon-avoidance criteria: instrument boresight cannot point within ζ of line-of-sight to the Moon due to stray-light constraints.

These combined constraints result in visibility restrictions for the spacecraft and instrument which are dynamic.

The scheduling terms used in this paper are defined as:

- Pointing: period of time that the instrument is inertially pointing to a region of the sky.
- Step: subset of a pointing focused on one target in the sky. A pointing is composed of a fixed number of steps.
- Large slew: a spacecraft maneuver to transition between successive pointings.
- Small slew: a spacecraft maneuver to transition between successive steps.
- Redundancy: number of times a given region of the sky is observed by the desired portion of the instrument FOV.

The observing scenario is described in terms of the number of pointings per orbit and number of steps per pointing.

3 Observing Scenario Strategy

The general all-sky observing strategy is to roughly point the spacecraft in the zenith direction in the orbit plane. Both the ascending and descending portions of the orbit are equally utilized for observing. This enables mapping of the entire celestial sphere because the orbital plane naturally precesses at a rate of 1 deg per day, enabling coverage of the entire celestial sphere in approximately 6 months. Furthermore, pointing in the zenith direction maximizes science efficiency because it maximizes the time between when the Earth-avoidance constraints will be violated. The required pointing direction for the instrument is generally selected to minimize the required spacecraft rotation, which is a function of the cant angle of the instrument relative to the spacecraft.

3.1 *Spacecraft and Instrument Configuration*

The instrument is fixed at an offset angle relative to the spacecraft boresight, see Fig. 1. To satisfy the Sun-avoidance constraint, the spacecraft tilts according to $\theta = \Omega - \beta$ as in Eq. (1). To satisfy the Earth-avoidance criteria in Eq. (2), the nod in the cross-track direction, δ, is constrained to:

$$\delta_{\max} \leq \cos^{-1}\left[\frac{\cos(\alpha)}{\cos(\theta)}\right]. \tag{3}$$

This restricts the time the instrument can focus at a single inertial target, where the maximum time is a function of half angle and the orbital period (where the following equation implicitly accounts for the conversion from degrees to radians),

$$T_{\max} = \frac{\delta_{\max} P}{\pi}, \tag{4}$$

where P is the orbital period and $\delta_{\max}$ is given in radians. The maximum pointing times, $T_{\max}$, vary as a function of β throughout the year. This places dynamic constraints on the problem; and as a result, the minimum number of pointings per orbit is higher for lower β values. An example is given in Fig. 2 for the SPHEREx mission described in the next section.

3.2 *Scheduling Algorithm*

The approach prioritizes the most constrained pointings and steps by scheduling them first, while also satisfying the dynamic constraints. Second, the all-sky algorithm generates a schedule

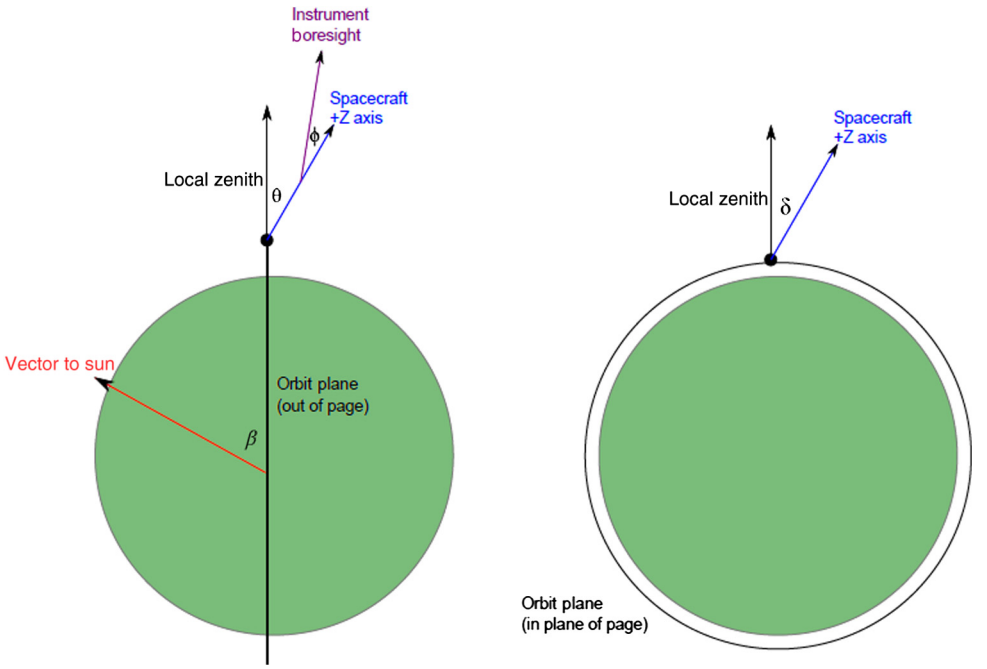

Fig. 1 Angle definitions for all-sky survey.

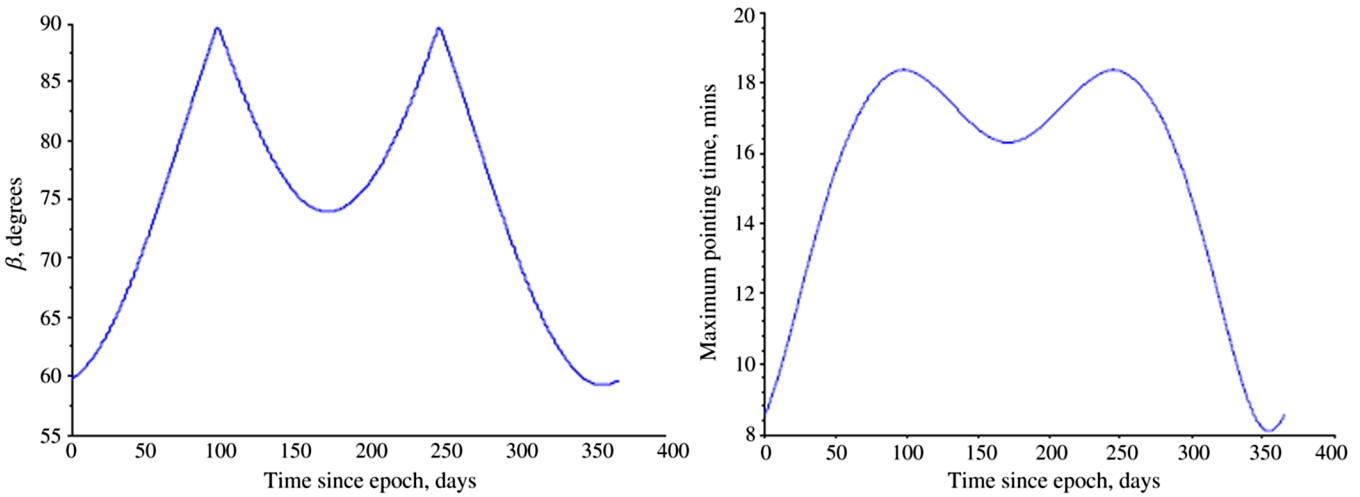

Fig. 2 The maximum pointing time is a function of the solar β angle as in Eq. (4).

that covers the complete celestial sky with the required redundancy in the planning horizon. The approach is constraint-based, thus by construction yields feasible solutions. Solutions are not guaranteed to be globally optimal for objectives such as maximizing science time or overall efficiency. However, solutions do provide good solutions and initial guesses for further scheduling optimization.

First, the targeted pointings are scheduled according to when they are accessible on the required cadence. Second, the all-sky pointings are scheduled, which is more complex and is described in greater detail next.

The following definitions are necessary to understand the algorithm pseudocode:

- T_s: Vector of starting times of all scheduled pointings.
- T_e: Vector of ending times of all scheduled pointings.
- $d(t)$: Vector of spacecraft orbit declinations, which are a function of time, t.
- D: Vector of required celestial declinations for the all-sky survey.
- RD: Vector of required number of steps to cover every declination in D, which depends on the planning horizon.
- SD: Vector of the scheduled number of steps for every declination in D.
- PD: Vector of declination indices of all scheduled pointings, corresponding to the times in T_e and T_s, with indices referring to the declinations in D.
- $n = |T_s| = |T_e| = |PD|$: number of scheduled pointings.
- s: Temporary variable indicating the number of steps in a given pointing.
- t_{sp}: Time duration of large slew between successive pointings.
- t_{ss}: Time duration of small slew between successive steps.
- t_{st}: Time duration of small step.
- τ: Temporary time variable representing the start of the next pointing.
- $\delta_{max}(\beta)$: the maximum tilt in the cross-track direction, which depends on β, as in Eq. (3).
- $T_{max}(\beta)$: the maximum pointing duration, which depends on β, as in Eq. (4).
- $F \subset D$: Vector of feasible declinations for a given scheduling opportunity.

Prior to applying the all-sky scheduling algorithm, the targeted observations are scheduled and assigned in T_s, T_e, and PD. To achieve complete coverage of the sky, each pointing is assigned a declination, and successive steps at that declination are taken by varying the RA, where the step size is equal to the desired FOV step size. Over time, the individual images stack up to achieve full coverage of each declination ring, as in Fig. 3. The successive images may overlap, depending on the instrument properties and survey requirements. For example, if the wavelength varies across the FOV, then successive FOV images will overlap to achieve the required wavelength resolution coverage. The all-sky pointings are scheduled according to a heuristic-based scheduling approach which can be applied to any planning horizon. The number of total required steps at each

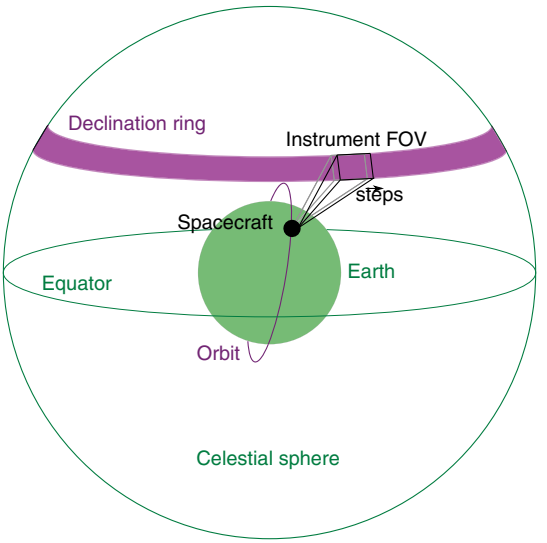

Fig. 3 Representation of the all-sky survey strategy, where the purple ring shows coverage along a region of constant declination, where on successive pointings, the field of view (FOV) is stepped sideways.

declination is a function of this planning horizon in order to achieve the required redundancy.

The algorithm for assigning the all-sky survey pointings is given in pseudocode below. The counter for the available gaps between targeted observations for scheduling all-sky pointings, i, and the counter for all scheduled pointings, j, are initialized in steps 1 and 2. The algorithm cycles through each available gap in the schedule and checks if there is sufficient remaining time for a single-step pointing (steps 3 and 4). If there is remaining time, the algorithm, which is the minimum of the time until the next scheduled pointing and $T_{\max}$ (constrained by β) are determined in step 9. Next, the declinations are identified that can be feasibly viewed throughout $T_{\max}$ (i.e., do not violate the Earth constraint at the start or end of the time interval) in step 10. The feasible all-sky declination with the maximum number of remaining steps is selected in step 11 and the number of feasible steps is computed in step 12. This prioritization supports equal coverage across all declinations. The declinations are assigned in steps 13 and 14. Finally, the starting and ending times of this and the next pointing are assigned. This process is repeated until every block of unassigned time is scheduled with all-sky pointings.

Algorithm Assigning all-sky pointings

1: $j \leftarrow n$
2: $i \leftarrow 0$
3: **while** $i < n$ **do**
4: $\quad i \leftarrow i + 1$
5: $\quad$ **if** $T_s(i+1) - T_e(i) \geq t_{\text{sp}} + t_{\text{st}}$ **then**
6: $\quad\quad \tau \leftarrow T_e(i) + t_{\text{sp}}$
7: $\quad\quad$ **while** $\tau \leq T_s(i+1) - t_{\text{sp}} - t_{\text{st}}$ **do**
8: $\quad\quad\quad j \leftarrow j + 1$
9: $\quad\quad\quad \Delta t \leftarrow \min[T_{\max}(\beta), T_s(i+1) - \tau - t_{\text{sp}}]$
10: $\quad\quad\quad F \leftarrow D$ s.t. $|d(\tau) - D| < \delta_{\max}$ & $|d(\tau + \Delta t) - D| < \delta_{\max}$
11: $\quad\quad\quad k \leftarrow \max[RD(F) - SD(F)]$
12: $\quad\quad\quad s \leftarrow \text{ceil}(\Delta t + t_{\text{ss}}/t_{\text{st}} + t_{\text{ss}})$
13: $\quad\quad\quad SD[F(k)] \leftarrow SD[F(k)] + s$
14: $\quad\quad\quad PD(j) \leftarrow D(k)$
15: $\quad\quad\quad T_s(j) \leftarrow \tau$
16: $\quad\quad\quad T_e(j) \leftarrow \tau + \Delta t$
17: $\quad\quad\quad \tau \leftarrow \tau + \Delta t + t_{\text{sp}}$
18: $\quad\quad$ end while
19: $\quad$ end if
20: end while $= 0$

The all-sky algorithm will append vectors T_s, T_e, PD, which will no longer be chronologically ordered because the algorithm fills in time periods without scheduled pointings (however, they can be easily sorted). This scheduling approach, including selection of the cadence and distribution of the targeted observations, as well as integration times for all surveys, should be iteratively applied, changing these design parameters until the appropriate values are determined to achieve the scheduling goals. In particular, the parameters should be selected such that all required all-sky pointings are accomplished (i.e., $SD = RD$), and that the desired trade-off between scheduling efficiency and redundancy for the targeted and all-sky pointings is achieved. This trade-off will have a great dependence on the location and number of targeted pointings, constraining the pointing opportunities for the all-sky survey. After the algorithm has been completed, the resulting schedule can also be improved; for example, short periods of time that remaining unscheduled can be reduced by increasing the number of steps (adding redundancy) or scheduling other spacecraft operations (e.g., downloads, reaction wheel de-saturation).

In practice, the slew times may deviate from the slew model, which the algorithm has inherent robustness to tolerate. In schedule implementation, each pointing will start to integrate only once the required pointing accuracy is acquired; therefore, if the slew time is less than expected, the integration time for the steps within that pointing will be longer and if the slew time is longer, than expected the integration times will be shorter. Overall, this strategy ensures the schedule achieves the required number of steps to satisfy the redundancy requirements over a given planning horizon; however, there may be a reduction or increase in integration time (and thus sensitivity) for different steps. The built-in schedule redundancy improves the strategy robustness toward accomplishing the science goals. The scheduling algorithm will be run with updated slew model parameters (and other scheduling parameters) based on performance to ensure optimal use of constrained time throughout the mission.

Completing the all-sky survey can be visualized as a gridded celestial sphere. When projected on an equal-area Mollweide map, as in Fig. 4, the circumference varies as a function of declinations, maximum at the equator and minimum at the poles due to the equal-area projection. To achieve global coverage with a redundancy of one in 6 months, a circumference of $c = 360 \text{ deg } \cos(d)$ must be covered for each declination, d. Thus, fewer steps are required near the poles relative to near the equator. The total number of steps to cover this area depends on the FOV size, number of required steps across the detector, and required redundancy.

4 Application to the SPHEREx Mission

This section applies the scheduling strategy and algorithm to the SPHEREx mission. SPHEREx is an astrophysics mission performing an all-sky spectroscopic survey, studying inflationary cosmology, the history of galaxy formation, and galactic ices. The SPHEREx spacecraft will be launched into a 500-km altitude Sun-synchronous (inclination = 97.4 deg) nearly terminator orbit (18 h orbit) with a period of 94.6 min, selected to minimize thermal concerns and maximize power collection with the ability to view the entire celestial sphere. This two-year mission is required to cover the entire celestial sphere once approximately every 6 months, the galactic plane once every 6 months, and maximize coverage of the north celestial pole (NCP) and south celestial pole (SCP) regions, as shown in Fig. 5.

In a nearly terminator Sun-synchronous orbit, the β angle varies between 60 deg and 90 deg throughout the year, see Fig. 2(a). The SPHEREx pointing constraints are: $\alpha \leq 35$ deg, $\zeta \leq 35$ deg, $\Omega = 90$ deg, thus $T_{\max}$ varies from 9 to 19 min throughout the year, see Fig. 2(b). For the SPHEREx spacecraft, ϕ is a fixed angle that must be determined before the spacecraft is developed (and impacts other subsystems such as thermal and attitude determination and control), while θ is a free decision

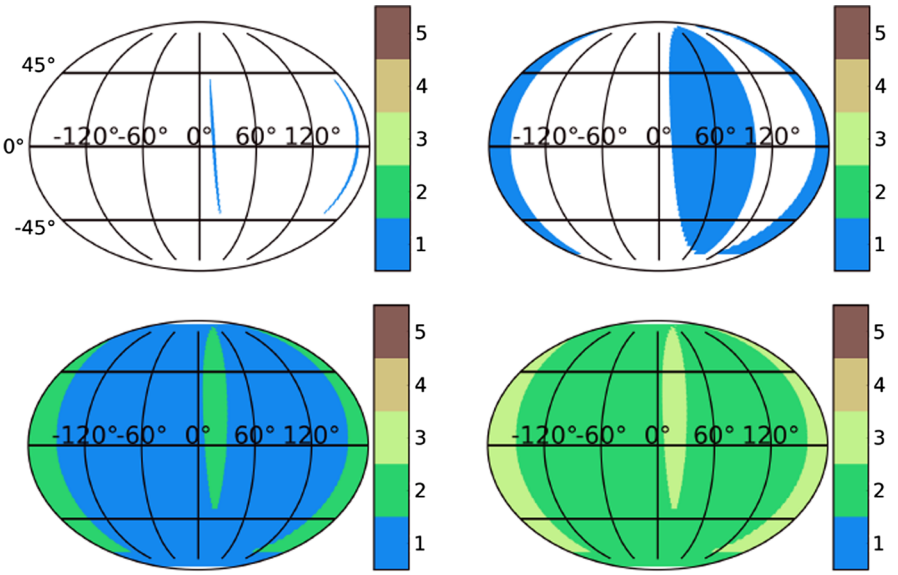

Fig. 4 Progressive coverage for all-sky survey, where the color shows the minimum wavelength coverage of every area of the sky. The approach achieves an overall efficiency of one in 6 months.

variable in the scheduling problem that is free to be dynamic over time.

4.1 *Survey Overview*

The three SPHEREx surveys focus on different areas of the celestial sky and have different integration and redundancy requirements. The deep survey consists of surveying 100 square degrees centered both at the NCP and SCP, respectively (which is assumed to be declinations ≤ -83.5 deg and ≥ 83.5 deg), as in Fig. 5. The NCP and SCP are selected as the deep survey regions because the poles are the natural rotation axis for the SPHEREx orbit and the instrument can access these regions throughout the year. The galactic plane survey requires coverage of approximately 1 deg above and below the galactic plane. The all-sky survey consists of the remaining celestial sphere and the full dataset will use data from the other surveys to achieve full celestial sphere coverage.

The SPHEREx instrument has a well-corrected FOV that is 7.04 deg by 3.52 deg, with the final image split by a dichroic plate to a pair of focal planes. There are two side-by-side detectors, each 3.52 deg square, in each focal plane as in Fig. 6. Immediately in front of each detector is a linear variable filter (LVF). These are wedge filters, where the coating thickness and thus, the transmitted central wavelength continuously vary along one dimension, oriented in the scan direction. The four LVFs span the wavelength range covered by the SPHEREx survey.[12]

The wavelength and spatial resolution requirements for the three surveys are given in Table 1. The all-sky and galactic plane surveys' requirements are the same, so the galactic survey is accomplished as part of the all-sky survey. Every survey requires complete wavelength coverage, meaning every wavelength (long rectangles in Fig. 6) FOV covers every area in the survey. Wavelength coverage is achieved by stepping the detector by the step required to achieve the required spectral resolution. In this mission application, redundancy is defined as the number of times a given area of sky is covered by every wavelength band applicable for that survey. The galactic and all-sky surveys require a redundancy of once per 6 months, meaning

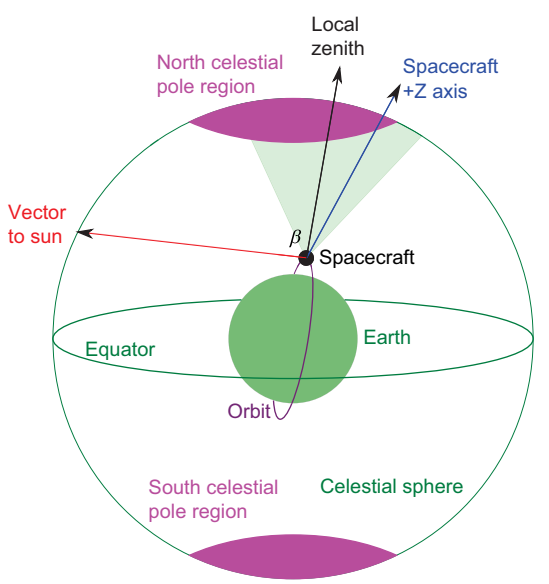

Fig. 5 Configuration and constraints for the SPHEREx mission.

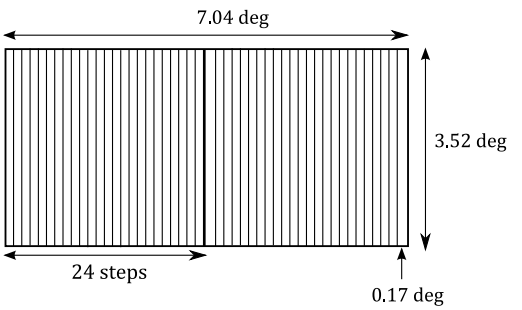

Fig. 6 Field of view (FOV) with 24 steps across each detector (as used for the all-sky and galactic plane surveys).

Table 1 SPHEREx survey overview.

Survey	Deep (NCP/SCP)	All-sky/ galactic plane
Parts of celestial sphere	NCP/SCP	All remaining sky
Spectral resolution	40	40
Steps across the detector	21	21
Integration time (per step)	185 s	95.7 s
Redundancy requirements	Maximized	once per 6 months

each half of the orbit (ascending and descending) covers the entire celestial sphere in view as it precesses. The scheduling objective is to maximize the redundancy of the deep surveys, i.e., uniformly sample the NCP and SCP and surrounding areas with the maximum number of times, subject to the requirements of all surveys.

The SPHEREx scheduling parameters are in Table 2, which are a function of the orbit altitude and inclination, FOV, and preliminary science, scheduling, and attitude control calculations. The slew times are the expected values over a 60 deg slew, however. in many cases (especially for $\beta < 90$ deg, where there are at least eight pointings per orbit), they will be considerably shorter, increasing integration times. Telecommunication operations require an average of 1.6 min per orbit, which is scheduled for about 7 min every three to four orbits. This telecommunication time is accounted for in the overall scheduling.

Due to its constraints, SPHEREx spacecraft boresight must point within the allowable regions shown in Fig. 7, constrained by both the Sun (edge closest to the Sun) and Earth (edge away from Sun).

4.2 *Spacecraft Configuration*

The instrument is at a fixed cant angle, ϕ, relative to the spacecraft (i.e., it cannot dynamically move throughout the orbit or

Table 2 SPHEREx schedule parameters.

Parameter	Values	Units
Orbits per day	15.2	orbits/day
Orbits per year	5552	orbits
Orbit period	94.7	mins
Orbit precession	1	deg/day
FOV half width	3.52	deg
All-sky/galactic integration time	95.7	sec
Deep (NCP/SCP) integration time	185	sec
Small slew duration (between steps)	10	sec
Large slew duration (between pointings)	90	sec
Telecom time	1.6	min/orbit

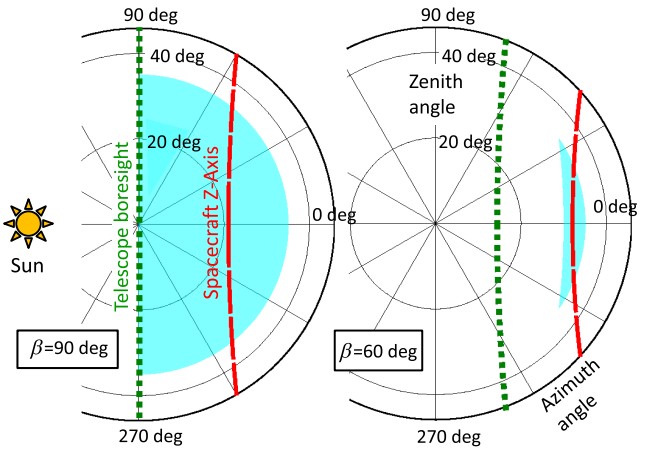

Fig. 7 Pointing constraints for the SPHEREx all-sky survey in a Sun-synchronous low Earth orbit (LEO) for different solar β values. The blue zone shows the regions where the spacecraft may point, where the edge closest to the Sun is due to Sun avoidance and the curved edge on the other side of the Sun is due to Earth avoidance.

year), which is a design variable that interacts with the observing scenario. In order for the instrument to have the NCP and SCP in view throughout the entire year, which is necessary to maximize the deep survey redundancy, and considering the tilt angle for solar avoidance (θ), $\phi = 21$ deg was selected. There is one limiting case throughout the year where either the NCP or SCP is on the edge of the FOV (i.e., a single wavelength range can image the NCP or SCP). A Sun-synchronous orbit with a longitude of descending node is 18 h is selected. As a result, the worst case occurs for the SCP during the winter solstice ($\beta = 60$ deg), as this pole has a lower priority. The worst case for the NCP is when the FOV is 2.4 deg from the NCP center, which occurs during the summer solstice ($\beta = 74$ deg).

For the $\beta = 90$ deg case, the angular difference between successive slews is generally about 60 deg (360 deg /6 pointings). Differences in successive pointing angles of up to approximately 80 deg can be tolerated (depending on the declinations), which exceeds the 75 deg that may be expected due to tilting from the local Zenith by 35 deg in each direction because of the motion of the spacecraft during the slew (about 90 s).

4.3 *Strategy Overview*

The SPHEREx mission is considered an "engineered" survey because the three survey goals are a natural synergy enabled by its polar orbit. Removing one of the surveys would not directly impact the other surveys, and in fact, as a result, the spacecraft may be idle for portions of the orbit. On every orbit, the instrument can access the NCP and SCP (enabled by the selection of the appropriate instrument cant angle ϕ), the galactic plane, and a band of the celestial sphere aligned with the orbit for all-sky survey coverage. In general, the surveys do not directly conflict because they target different areas of the celestial sphere; however, there are trade-offs between the various surveys.

The overall strategy maximizes science time by minimizing the number of pointings because the large slew durations are longer than the small slew durations, see Table 2. However, the pointing durations must never exceed $T_{\max}$, see Fig. 2(b), so when $\beta = 60$ deg, at least eight pointings are required,

and when $\beta = 90$ deg, at least six pointings are required. Figure 8 shows a representative distribution of pointings throughout an orbit for the $\beta = 90$ deg, where there is one NCP, one SCP, and four all-sky pointings (which also cover the galactic plane) per orbit. The number of arrows represents the number of steps per orbit, and an example is given to satisfy the Moon-avoidance constraint. The distribution of number and location of pointings and steps will vary depending on β, location of the galactic plane, Moon, and specific orbit.

To achieve full wavelength coverage for the all-sky survey, successive pointings will pick up where the last pointing left off such that the individual images stack and achieve full wavelength coverage, as in Fig. 3. For the SPHEREx mission, when $\beta = 90$ deg, there are a total of 367 all sky steps that must be accomplished per day, or approximately 24 steps per orbit to account for covering both the ascending and descending sides of the orbit, which is sufficient for achieving global coverage. The number of required steps per orbit is driven by the Earth and Sun constraints. The number of steps to achieve global coverage is always lower, thus satisfied. This is true in both extreme cases, when $\beta = 60$ deg (with at least eight pointings per orbit and four steps/pointing), and when $\beta = 90$ deg (with at least six pointings per orbit and six steps/pointing). However, if the redundancy requirement increases or the number of steps/pointing dramatically changes, this may introduce new constraints. The galactic and all-sky surveys have the same wavelength and redundancy requirements, as in Table 1, thus the galactic science is accomplished as part of the all-sky survey. In the case that the galactic survey wavelength or redundancy requirements differ, an alternative approach may be required, as discussed in Sec. 4.5.

To maximize the deep survey observations, there is an NCP and SCP pointing on a large number of orbits. The spacecraft will not perform observations of NCP and SCP regions on every orbit because they would conflict with high-declination all-sky observations; therefore, we skip these deep sky observations on some fraction of orbits. For example, see the fractions in Table 3 for the $\beta = 90$ deg case. Efficient coverage of the polar caps is achieved by stepping the FOV along lines of constant RA for a given number of steps, and repeating the pattern at the next RA once the orbit has precessed. To achieve uniform coverage over the deep region, the number of steps at each declination will not be exactly even. In addition, there will be incomplete wavelength overhang (regions of the sky that are covered by the FOV when completing the edges of the deep region) on to the all-sky survey that will augment its coverage but will not be part of the deep survey.

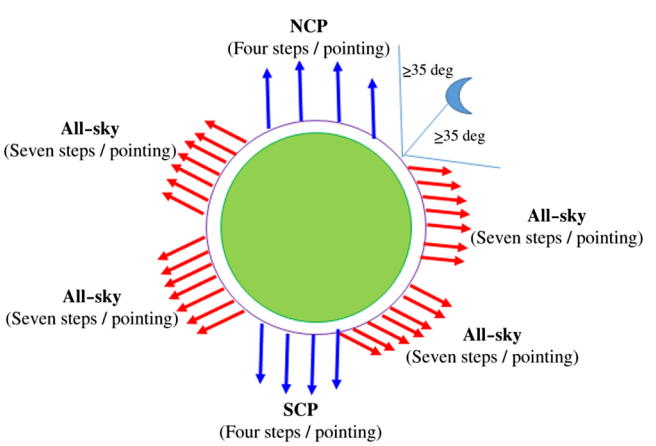

Fig. 8 Idealized general observing scenario for $\beta = 90$ deg case where there are six pointings per orbit.

Table 3 Representative ideal schedule overview for $\beta = 90$ deg with the scenario parameters in Table 2.

Parameter	Deep (NCP/SCP) Survey	All-sky Survey	Total	Units
Pointings per orbit (average)	2	4	6	pointings
Pointings per year (average)	11104	22207	33311	pointings
Steps per pointing (average)	4	7		steps
Steps per orbit (images per orbit)	8	28	36	steps
Steps per year	44414	15545	199865	steps
Integration time per step	185	99		secs
Science time	1660	3156	4816	secs
Percentage of science time	34.5	65.5	100	%
Total time (including small slews)	28.7	56.6	85.3	mins
Large slews			7.5	mins
Telecommunication time			1.6	mins
Total scheduled time (including small slews)			93.6	mins
Science efficiency			84.7	%

Table 3 provides an idealized summary of the three surveys, pointings, and steps for the representative $\beta = 90$ deg case, which is shown in Fig. 9(a). This case assumes perfect scheduling (i.e., every second is scheduled) and overall average number of pointings and steps (which is why there are fractional values where pointings and steps would nominally be integers). Overall, 84.7% of the time is dedicated to science observations, with the largest fraction of other time dedicated to large slews (five 90 s slews).

4.4 *Scheduling Algorithm Implementation*

The algorithm described in Sec. 3.2 is applied to the SPHEREx mission, where the targeted observations focus on the deep survey regions. The survey is implemented in MATLAB® with orbital information generated with the Systems Tool Kit (STK)®. The algorithm was applied to realistic SPHEREx scenarios and the resulting schedules are shown in Figs. 9 and 10. The schedule is applied to two-day planning horizons, during which time the all-sky survey steps fully cover 2 deg in RA, as the orbit precesses at 1 deg per day. The binned number of steps per day at each declination is shown in Fig. 11, which is essentially the total number of stacked steps from Fig. 9. To satisfy all surveys, we converged to a cadence of NCP/SCP pointings (each with four steps) for three out of every four orbits

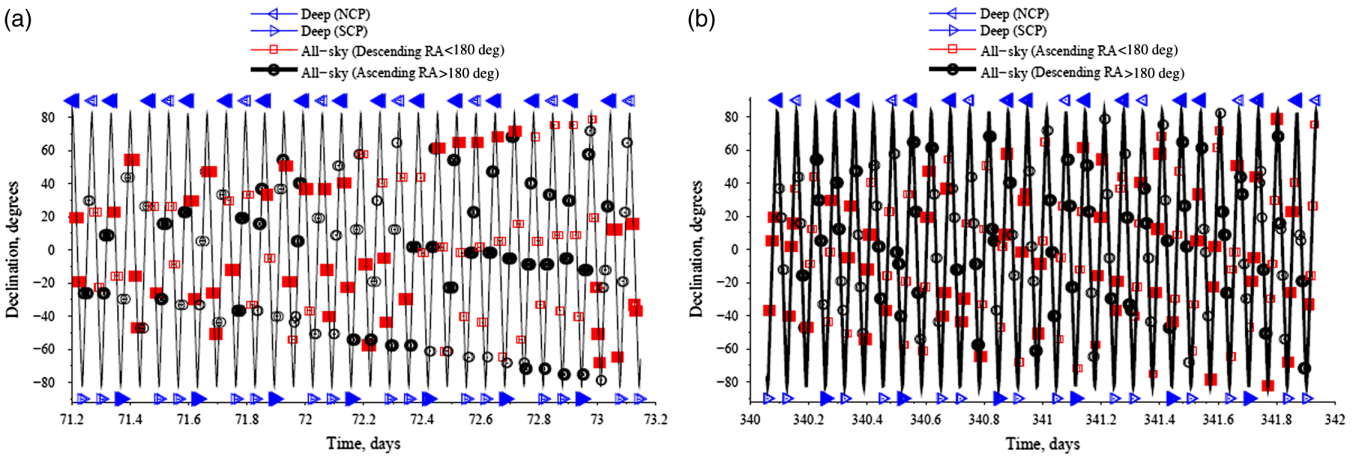

Fig. 9 (a,b) Representative schedules for a two-day planning horizon. The black solid lines denote the orbit track on the celestial sphere, which establishes the available declinations as a function of time. The symbols denote the survey pointings, which are chosen to satisfy the constraints, where each pointing is comprised of 4 to 9 steps where the step duration depends on the survey type. There are large slews (90 s) between successive pointings and small slews (10 s) between successive steps (in a single pointing) not shown here.

when $\beta = 90$ deg, and for two out of every three orbits when $\beta = 60$ deg. This solution provides good science efficiency and satisfies the all-sky survey requirements.

As expected, the schedule results in six pointings/orbit for the $\beta = 90$ deg case and eight pointings/orbit for the $\beta = 60$ deg, which emerged naturally from the algorithm (i.e., it was not prespecified). The telecommunication operations (downloading and uploading from Earth ground stations) are not shown in Figs. 9 and 10 because they only occur a few times a week; however, appropriate time is allocated to these operations in the average time allocations, see Table 3. As the orbit precesses, a similar schedule is repeated at different RAs to cover the celestial sphere.

Implementing the schedule for the $\beta = 90$ deg case, as shown in Figs. 9 and 10, results in a science efficiency of 78%. This efficiency could be improved by using the generated schedules as initial guesses in a global optimization problem with more decision variables and model improvements. Decision variables such as the NCP/SCP pointing cadence, placement in the schedule, and/or total number of pointings could be used in the optimization formation toward improving scheduling flexibility and maximizing efficiency. Model improvements could reduce the conservatism of the current approach and improve accuracy and efficiency of the resulting schedules. For example, the slew times could be modeled more accurately based on actual slew angles for both short and long slews and the problem could be constrained to prevent any down time between science observations and slews.

Representative coverage visualizations of the all-sky survey over long-duration planning horizons are shown in Fig. 4. The observing scenario strategy achieves the required redundancy requirements for the all-sky survey after 7 months. The reason

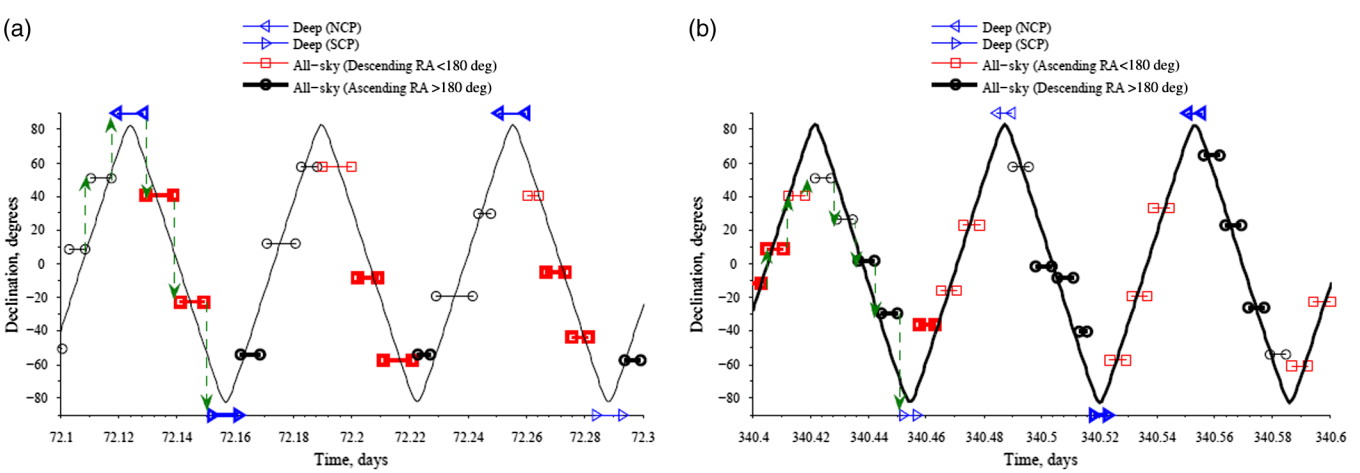

Fig. 10 Representative schedules for three orbits (detailed view of the schedules in Fig. 9). The black solid lines denote the orbit track on the celestial sphere, which establishes the available declinations as a function of time. The green dotted lines with arrows denote the large slews between successive pointings. The symbols denote the survey pointings, which are chosen to satisfy the constraints, where each pointing comprised 4 to 9 steps where the step duration depends on the survey type. There are large slews (90 s) between successive pointings are shown in green dotted lines, and small slews (10 s) between successive steps (in a single are pointing) are not shown here.

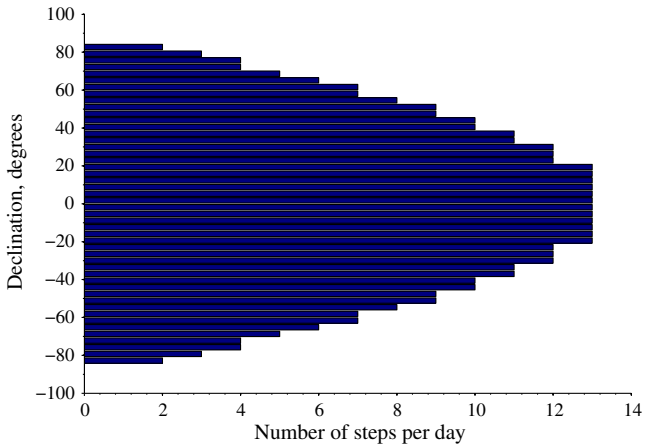

Fig. 11 (a,b) Histogram of idealized number of steps per day to achieve redundancy requirements for all-sky survey. This distribution in declination is readily implemented by the scenario illustrated in Fig. 9.

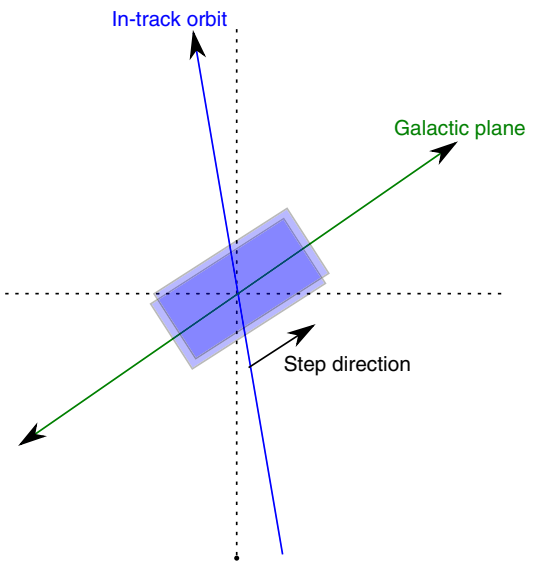

Fig. 12 Steps along the galactic plane to achieve complete coverage.

for the inability to accomplish completely uniform coverage in 6 months and the triangular regions that show nonuniform coverage at 7 months are due to the inclination of the orbit and the desire to minimize spacecraft tilting to maximize pointing durations.

4.5 *Special Case: Galactic Plane Survey*

To demonstrate how a targeted observation can be accommodated in the SPHEREx observing strategy and because of the scientific interest in the galactic plane, we address the special case where in addition to the all-sky survey, the mission must include coverage of the galactic plane with higher spatial resolution or redundancy than the rest of the survey. In a LEO, the RA where the spacecraft crosses the galactic plane varies throughout the year, so the orbit declination where the orbit crosses the galactic plane is also dynamic. The spacecraft has two opportunities to image every part of the galactic plane every year due to the orbital precession, which provides some flexibility on when galactic plane pointings are scheduled.

The galactic plane runs at an angle relative to the orthogonal lines of RA and declination. To efficiently cover this area, the proposed strategy is to rotate the spacecraft such that the long end of the instantaneous FOV is parallel to the galactic plane and the FOV is centered at the galactic plane. Thus, successive steps along the galactic plane with the required step size are necessary to achieve full coverage, as shown in Fig. 12. The number of steps required to cover the galactic plane depends on the FOV and the redundancy requirements. The ability to rotate the spacecraft may be constrained by solar panel or star tracker angles, or thermal limitations.

5 Conclusion

This paper presented an approach for scheduling all-sky surveys that accommodates targeted observations subject to challenging constraints in the LEO environment. The approach includes spacecraft and instrument constraints related to dynamic and interacting thermal and stray-light environments, which vary as a function of the orbit position relative to the Sun, Earth, and Moon. The instrument and spacecraft configuration problem is solved to satisfy the Sun-avoidance criteria, which combined with the Earth-avoidance criteria, leads to dynamic maximum observation time constraints throughout the year. Targeted observations constrain the opportunities for all-sky observations. A heuristic-based all-sky scheduling algorithm is presented that is designed to generate guaranteed-feasible solutions that achieve the all-sky redundancy requirements. The approach is applied to the proposed SPHEREx mission, which consists of a deep survey focusing on the celestial poles and an all-sky survey including a galactic plane survey, where each survey has specific requirements and objectives. Representative solutions are presented that achieve the survey goals for nominal and worst-case scenarios. The all-sky survey scheduling efficiency of the implemented algorithm is approximately 78%, while idealized schedules achieve an efficiency of approximately 85% ($\beta = 90$ deg case). Methods to optimize the solutions and to maximize science efficiency are presented.

Beyond the approach for efficiently accomplishing all-sky surveys, this paper presents insights for operating a spacecraft in the challenging LEO environment, where there may be Sun-, Earth-, and Moon-avoidance constraints. Furthermore, this approach could be utilized to map the Earth with nadir-pointing spacecraft instead of the celestial sphere with a zenith-pointing spacecraft. The step-wise approach of solving several subproblems presented in this paper has significantly reduced the number of constraints, variables, and objectives. This approach is applicable to a larger class of spacecraft scheduling problems.

Acknowledgments

The authors acknowledge Olivier Dore, Timothy Kock, Kirk Breitenbach, Hemali Vyas, Dustin Crumb, and Anthony Pullen for their contributions. Part of the research was carried out at the Jet Propulsion Laboratory, California Institute of Technology, under a contract with the National Aeronautics and Space Administration.

References

1. J. G. Emming et al., "Pulse circumvention circuit for the infrared astronomical satellite telescope," *Proc. SPIE* **0445**, 254–263 (1984).

2. "Infrared Astronomical Satellite," Infrared Processing and Analysis Center, Science and Data Center for Infrared Astronomoy, http://www.ipac.caltech.edu/project/15 (2015).
3. W.-S. Jeong et al., "ASTRO-F/FIS observing simulation including detector characteristics," *Adv. Space Res.* **34**(3), 573–577 (2004).
4. "Operation Plan," AKARI (ASTRO-F; Infrared Imaging Surveyor), 2005, http://www.ir.isas.jaxa.jp/ASTRO-F/Outreach/unyou_e.html (2015).
5. E. W. Wright et al., "The wide-field infrared survey explorer (wise): mission description and initial on-orbit performance," *Astron. J.* **140**, 1868 (2010).
6. "WISE Mapping the Infrared Sky," 2010, http://wise.ssl.berkeley.edu/documents/FactSheet.2010.1.4.pdf (2015).
7. "ROSAT All Sky Survey Data: A Guide for Non-Expert users," ROSAT Guest Observer Facility, 2012, http://heasarc.gsfc.nasa.gov/docs/rosat/rass.html (2015).
8. J. W. Gangestad et al., "A high earth, lunar resonant orbit for lower cost space science missions," *Earth Planet. Astrophys.* (2013).
9. M. D. Johnston, e. M. Z. G. E. Miller, and M. K. M. Fox. San Mateo, "Spike: intelligent scheduling of Hubble space telescope observations," *Intell. Scheduling* 391–422 (1994).
10. M. E. Giuliano and M. D. Johnston, "Multi-objective evolutionary algorithms for scheduling the James Webb space telescope," in *Proc. Int. Conf. on Automated Planning and Scheduling (ICAPS)*, Sydney, Australia (2008).
11. M. E. Giuliano and M. D. Johnston, "Multi-objective evolutionary algorithms for scheduling the James Webb space telescope,"in *Proc. Eighteenth Int. Conf. on Automated Planning and Scheduling (ICAPS 2008)* (2008).
12. K. Rosenberg et al., "Logarithmically variable infrared etalon filters," *Proc. SPIE* **2262**, 25–27 (1994).

Sara C. Spangelo received her PhD in aerospace engineering at the University of Michigan in 2012 focusing on optimizing small spacecraft networks, where she was involved in the RAX CubeSat missions. She has consulted on model-based approaches to design and operates spacecraft and high-altitude balloons. At the NASA Jet Propulsion Laboratory (JPL), she has been a lead systems engineer for mission concepts ranging from discovery-class to interplanetary CubeSats. Her research focuses on optimizing vehicles and trajectories for interplanetary small spacecraft constellations.

Raj M. Katti will begin a PhD in physics at the California Institute of Technology in 2015. Prior to his graduate studies, he worked as a research technician in the Caltech Observational Cosmology group led by professor Jamie Bock. His work in professor Bock's group has focused on survey design and visualization for SPHEREx and detector analysis for the BICEP program.

Stephen C. Unwin is a principal scientist at the Jet Propulsion Laboratory in Pasadena, California. He received his PhD in radio astronomy from the University of Cambridge, and was a postdoc at Caltech before moving to JPL. His research interests include relativistic jets and broad-band energy distributions in active galactic nuclei, and space instruments and mission architectures for the direct detection and spectroscopy of extrasolar planets.

James J. Bock (California Institute of Technology and the Jet Propulsion Laboratory) received his BS degrees in physics and mathematics from Duke University in 1987 and his PhD in physics from UC Berkeley in 1994. He has developed instrumentation for studying the polarization of the cosmic microwave background and the spatial and spectral properties of the near-infrared extragalactic background. As the US PI, he led the focal plane detector development for the Herschel/SPIRE and Planck/HFI satellites.